Potential Energy Function for Intramolecular Proton Transfer Reaction of Glycine in Aqueous Solution

Naoto Okuyama-Yoshida[†,‡] and Masataka Nagaoka*

Institute for Fundamental Chemistry, 34-4, Takano-Nishihiraki-cho, Sakyo-ku, Kyoto 606, Japan

Tokio Yamabe

Division of Molecular Engineering, Kyoto University, Sakyo-ku, Kyoto 606, Japan

Received: September 24, 1997[⊗]

An analytical potential function of the glycine−water system, which can describe not only a reactive potential energy surface but also the interaction energy with water, has been proposed, by the empirical valence bond method with the exchange matrix element improved by Chang and Miller to reproduce an *ab initio* molecular orbital (MO) surface with high accuracy. The fitted potential function can reproduce satisfactorily the Born−Oppenheimer adiabatic surface obtained by *ab initio* MO calculations. Further, by molecular dynamics (MD) simulation and the free energy perturbation theory, we have presented the average of the interaction energy of glycine with water and the free energy profile of its intramolecular proton transfer reaction along the intrinsic reaction coordinate. It has been found that the zwitterionic form of glycine is much more stable than the neutral form, which is consistent with the result of Clementi et al. We obtained the free energy change of the reaction and that of activation to be 8.46 and 16.85, kcal/mol, respectively, which are in good agreement with the experimental values. We conclude that our potential function can work very well for the MD simulations of the chemical reaction.

I. Introduction

Glycine is the smallest amino acid, and there is considerable interest in the structure, reactivity, and other properties because of its pivotal biological significance.[1,2] The structures of the molecule are completely different in the gas phase and aqueous solution. According to *ab initio* electronic structure investigations,[3−5] in the gas phase, glycine is a nonionic molecule, and a glycine zwitterion (ZW) does not exist stably. Recently, Jensen and Gordon[6] have investigated how many water molecules are needed in order to stabilize the ZW in the gas phase by *ab initio* MO methods and found that two water molecules stabilize the ZW and then it becomes a minimum on the potential energy, adiabatic ground state, and 298 K free energy surface.

On the other hand, by using the titration method, Wada *et al.*[7] concluded that the ZW is much more stable than the neutral form (NF) of glycine in water solution by the free energy change 7.27 kcal/mol. Further, by determining the ratios of the ZW to the NF in the mixtures of water with the organic solvents, they concluded that the free energy change of the intramolecular protonation process in glycine is controlled mainly by electrostatic interaction, especially by the entropy change associated with the preferential solvation around the charged amino and carboxyl groups. According to Monte Carlo (MC) simulations,[8−10] in aqueous solution, the ZW is much more stable than the NF by the interaction energy change 86.4 kcal/mol. Therefore, the potential energy surface of glycine will vary drastically as its environment changes from the gas phase to aqueous solution. In other words, it is difficult to imagine the transition state (TS) structure of the reaction from the ZW to the NF in aqueous solution, although at least we could predict that it is different very much from both structures of the ZW in aqueous solution and the NF in the gas phase.

There are many studies on kinetics of the intramolecular proton transfer reaction of glycine in aqueous solution.[11−16] By various NMR relaxation techniques,[11,12] the rate constant of 175 s^{-1} was obtained. By the chemical relaxation method, Slifkin and Ali[13] obtained the free energy of activation of 14.36 kcal/mol. Furthermore, with the determination of the rate constant at several temperatures, they derived enthalpy and $-T\Delta S$ contributions to the free energy of activation of −0.22 and 14.57 kcal/mol, respectively.[13] On the other hand, the rate constant of the reverse reaction from the NF to the ZW is 4.4×10^7 s^{-1} and much faster than the former.[1,11−13] For the reverse reaction, it may be expected that the solvent molecules hardly have a chance to equilibrate with the reactant. In other words, the equilibrium assumption may be invalid, on which the conventional transition state theory (TST)[17−19] is based. In such cases, the rate constant will deviate from the TST rate constant due to the nonequilibrium distribution of state.[20−25] If we knew the TS structure in aqueous solution, it might enable us to estimate how far from equilibrium the nonequilibrium distribution is and how much the rate constant deviates from the TST one by the molecular dynamics (MD) simulation. In addition, it should be noticed that, although the most stable conformations of the ZW have been obtained in the studies on the conformation analyses in the gas phase[26] and aqueous solution,[27] respectively, a true TS in aqueous solution, i.e., the TS on the free energy surface, has never been determined.

For the purpose of pursuing the TS structure in aqueous solution, we need such a reactive potential energy function that reproduces a potential surface of glycine globally. Moreover,

* Author to whom correspondence should be addressed.
† Permanent address: Daicel Chemical Industries, LTD., 1239, Shinzaike, Aboshi-ku, Himeji, Hyogo 671-12, Japan.
‡ Also associated with the Division of Molecular Engineering, Kyoto University, Kyoto 606, Japan.
⊗ Abstract published in *Advance ACS Abstracts,* December 1, 1997.

S1089-5639(97)03102-2 CCC: $15.00
Published on Web 01/01/1998

the potential energy function should describe well the interaction energy among the solute and solvents in the course of the reaction, because the charge distribution of glycine drastically changes and the reaction environment is altered by the electrostatic interaction of glycine with surroundings as the reaction proceeds. There have been so many studies on reactive potential energy functions;[28−31] for example, the LEPS potential function[28] has been often employed, since it is based on a quantum mechanical description of the electronic wavefunction. However, it can only deal with triatomic or tri-pseudo-atomic surface. Therefore, we cannot adapt it to glycine, because it contains too many atoms (10 atoms). Nagaoka *et al.*[29] have succeeded in constructing the reactive potential function that describes the proton transfer reaction of formamidine−water system in aqueous solution, although the system degrees of freedom are as many as those of glycine. However, since the interaction potential energy function between the solute and solvents does not change during the course of the reaction, it also cannot be applied to glycine whose charge distribution should drastically vary in the course of the reaction.

There is an approach that can describe both many degrees of freedom and the changing of the interaction energy between a solute and solvents as a reaction proceeds. Warshel *et al.*[30] have designed and developed the approach in order to model reactive potential functions. It is called the empirical valence bond (EVB) model. Recently, the efficiency of the EVB model has been examined by Chang and Miller[31] who improved the analytical form of the exchange matrix element and found that gas-phase *ab initio* MO surfaces can be reproduced with high accuracy. The EVB method uses the valence bond (VB)[32] concept with respect to ionic−covalent resonance to obtain the Hamiltonian for an isolated reactive molecule and then evaluates the Hamiltonian for the reaction in solution by adding the calculated solvation energies to the diagonal matrix elements of the ionic resonance forms.[30] In the present work, we will apply the EVB method to the intramolecular proton transfer reaction of glycine in aqueous solution and construct a reactive potential energy function that describes the potential energy surface of the reaction globally.

The present paper is organized as follows. After introducing the EVB and MD methods and the free energy perturbation theory[33−36] in section II, we will show in section III to what extent the potential energy function is fitted to the *ab initio* data. Furthermore, in order to examine how well the potential function reproduces the interaction of glycine with surroundings, i.e., water molecules, by means of MD simulation and the free energy perturbation theory, we will present the averages of the interaction energy and the free energy changes for the present reaction along the intrinsic reaction coordinate (IRC). Finally, the main results are summarized in section IV.

II. Methodology

A. EVB Method. Let us consider the intramolecular proton transfer reaction of glycine in the gas phase such as

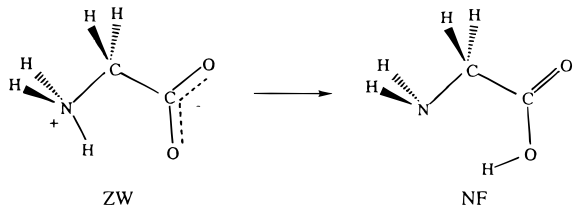

(2.1)

In the language of the VB theory,[32] the potential energy surface for the molecule results from mixing of the above two resonance forms, i.e., the ZW and NF. Therefore, the two-state VB electronic wave function can be written as follows

$$|\psi\rangle = c_1 |\phi_1\rangle + c_2 |\phi_2\rangle \tag{2.2}$$

where $|\phi_1\rangle$ is a VB wave function that describes the electronic structure of the ZW in eq 2.1 and $|\phi_2\rangle$ is the corresponding wave function that describes the electronic structure of the NF. The lowest electronic eigenvalue, i.e., the ground-state potential energy surface, is obtained by diagonalizing the Hamiltonian H_{el} and is then given by[31]

$$V_R = \frac{1}{2}(V_{11} + V_{22}) - \sqrt{\left(\frac{V_{11} - V_{22}}{2}\right)^2 + V_{12}^2} \tag{2.3}$$

where

$$V_{11} = \langle\phi_1|H_e|\phi_1\rangle \tag{2.4}$$

$$V_{22} = \langle\phi_2|H_{el}|\phi_2\rangle \tag{2.5}$$

$$V_{12} = \langle\phi_1|H_{el}|\phi_2\rangle \tag{2.6}$$

and R denotes "reactant". The diagonal matrix elements of the Hamiltonian, i.e., V_{11} and V_{22}, have such clear physical meaning that they are the energies of the related resonance forms. According to Warshel,[30] we can assume the analytical forms of V_{11} and V_{22} rather simply by making use of appropriate molecular mechanical potentials. We have actually employed the AMBER potential function[36] as follows

$$V_{kk} = \sum_{\text{bonds}} K_r(r - r_{eq})^2 + \sum_{\text{angles}} K_\theta(\theta - \theta_{eq})^2 + \sum_{\text{dihedrals}} \frac{K_\phi}{2}[1 + \cos(n\phi - \gamma)] + \sum_{i>j}\left(\frac{A_{ij}}{r_{ij}^{12}} + \frac{B_{ij}}{r_{ij}^{6}} + \frac{C_{ij}}{r_{ij}}\right) + \sum_{\text{H-bonds}}\left(\frac{D_{ij}}{r_{ij}^{12}} - \frac{E_{ij}}{r_{ij}^{10}}\right) \quad (k = 1, 2) \tag{2.7}$$

where r, θ, ϕ, and r_{ij} are bond lengths, bond angles, dihedral angles, and interparticle separations between the ith and jth atoms, respectively, and r_{eq}, θ_{eq}, K_r, K_θ, K_ϕ, γ, A_{ij}, B_{ij}, C_{ij}, D_{ij}, and E_{ij} are disposable parameters. Since we have not adopted the AMBER parameters themselves in order to make the function simpler, the parameters were fitted to the *ab initio* data under the following conditions: $n = 1$, and γ, D_{ij}, and E_{ij} equal to zero. From physical intuition, it is easy to understand that the following additional conditions must be fulfilled: $K_r > 0$, $K_\theta > 0$, and $A_{ij} > 0$.

The most crucial part of the EVB model is the exchange matrix element V_{12}, for it is ambiguous how its form should be chosen. Warshel has approximated it by an exponential form and fitted the parameters to experimental results on both the gas-phase potential energy surface and the free energy surface in solution, while Chang and Miller (CM)[31] have recently improved the analytical form for the square of the exchange matrix element (SEME), i.e., V_{12}^2, as follows

$$V_{12}^2 = A\cdot\exp\left(B^T\Delta\mathbf{q} - \frac{1}{2}\Delta\mathbf{q}^T C\Delta\mathbf{q}\right) \tag{2.8}$$

so that *ab initio* surfaces can be reproduced with high accuracy. In eq 2.8, $\Delta\mathbf{q} = \mathbf{q} - \mathbf{q}_0$, where $\mathbf{q}$ and $\mathbf{q}_0$ denote any geometry and the reference geometry, i.e., for instance, the TS structure,

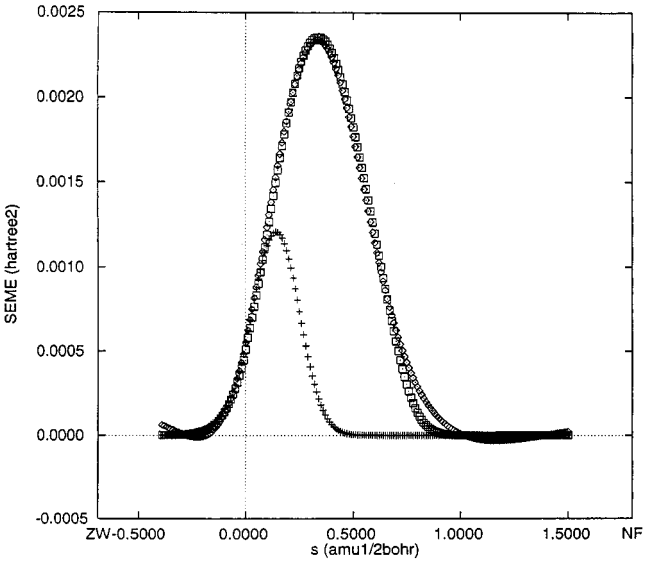

Figure 1. SEMEs by the CM's method (plus) and the present procedure (open square) and their corresponding quantum mechanically calculated values (open diamond). The abscissa is the IRC.

respectively, in terms of internal coordinates. Furthermore, *A*, *B*, and *C* are a disposable constant, vector, and matrix, respectively. According to CM,[31] *A*, *B*, and *C* should be determined so that the potential function should reproduce the *ab initio* potential with respect to not only the value of potential energy but also the force vector and Hessian matrix at an *ab initio* TS. The SEME determined by the CM's method can reproduce the corresponding *ab initio* MO values in the vicinity of the glycine TS very well. However, in the region remote from the TS, it deviates from the *ab initio* data very largely (see Figure 1). Therefore, it has been fitted with respect to *A*, *B*, and *C*, using all sample points in order to describe the potential surface not only in the vicinity of the TS but also at various points in the neighborhood along the IRC,[37] because the IRC should play a central role in chemical reaction ergodography.[37]

So far, we have discussed the reaction in gas phase. Next, let us consider to include the solvent, i.e., water molecules, which surrounds the reactive solute: glycine. The EVB method can also evaluate the Hamiltonian for the reaction in solution by adding the solute−solvent interaction energies to the diagonal matrix elements.[30] Solving the lower root of the 2 × 2 secular equation similarly, we can obtain the potential energy surface of glycine which contains the interaction energy as follows

$$V_{RS} \frac{1}{2}(V_{11} + V_1^{int} + V_{22} + V_2^{int}) - \sqrt{\left(\frac{V_{11} + V_1^{int} - V_{22} - V_2^{int}}{2}\right)^2 + V_{12}^2} \quad (2.9)$$

where V_1^{int} and V_2^{int} are the interaction energy between the ZW and water, and that between the NF and water, respectively, and R and S denote "reactant" and "solvent", respectively. Although so many analytical forms of the interaction energy have been investigated,[8−10,23,38] in order to apply them to our system, they must necessarily contain the Coulomb potential term, because the ZW consists of positively charged amino and negatively charged carboxyl groups and has a very large dipole moment (10.80 D at HF/6-31+G*). Therefore, we have employed the following form that Clementi et al.[8−10] have developed, so as to make the function as simple as possible,

$$V_k^{int} = \sum_n^{\text{solute}} \sum_i^{n\text{th water}} \sum_j \left(\frac{A_{ij}^{int(k)}}{R_{ij}^{12}} + \frac{B_{ij}^{int(k)}}{R_{ij}^{6}} + \frac{C_{ij}^{int(k)}}{R_{ij}}\right) \quad (k = 1, 2) \quad (2.10)$$

where R_{ij} is the distance between the *i*th atom on the solute and the *j*th atom on the *n*th water molecule, and $A_{ij}^{int(k)}$, $B_{ij}^{int(k)}$, and $C_{ij}^{int(k)}$ are disposable parameters. From a physical point of view, we have postulated that $A_{ij}^{int(k)} > 0$.

Finally, we have employed the TIP4P model[39,40] for solvent−solvent interaction potential V_{SS}, where S denotes "solvent", because the model has a simple analytic form and gives reasonable structural and thermodynamic descriptions of liquid water. Therefore, the total potential function V_{tol} of glycine−water system is as follows:

$$V_{tol} = V_{RS} + V_{SS} \quad (2.11)$$

B. Sample Points and Optimization Procedure. To optimize the above mentioned disposable parameters, *ab initio* SCF MO calculations have been performed at the HF/6-31+G* level of theory, using the GAUSSIAN92 program.[41] The relatively small basis set has been employed because the calculations of electronic energies and forces are necessary at so many points, i.e., 5250 points (97 points for V_{11}, 97 points for V_{22}, 2236 points for V_{12}^2, a couple of 1410 points for V_1^{int} and V_2^{int}), and the extremely small barrier height of 0.563 kcal/mol should be considered in good agreement with such results that there is no minimum corresponding to the ZW in the gas phase[4,5] for some larger basis sets than 6-31+G* and the post-SCF MO theory.

For the *diabatic* potential functions V_{11} and V_{22}, corresponding to two minima, i.e., the reactant and product, respectively, we have sampled 48 [24 (the degrees of freedom) × 2] points along the displacement vectors of the normal coordinates to the extent of 0.298 kcal/mol [$=k_BT/2$ (T = 300 K)] and 48 points to the extent of 0.596 kcal/mol [$=k_BT$ (T = 300 K)], i.e., totally 97 points [48 × 2 + 1 (minimum geometry)], at each minimum.

For the SEME V_{12}^2, the energies have been calculated at various points in the neighborhood along the IRC.[37] That is, we chose 22 points on the IRC at regular intervals, including the reactant, TS, and product geometries. Further, for a simple but effective method that enables us to sample geometrical points for *ab initio* energy calculations at each point on the IRC, we have utilized the normal mode vectors[42] perpendicular to the IRC. These vectors are obtained at each point on the IRC by diagonalizing the projected force constant matrix that does not include those degrees of freedom for the IRC, overall translation, and rotation. We have sampled 46 [{24 (the degrees of freedom) − 1 (the degree of freedom of IRC)} × 2] points along the normal mode vectors to the extent of 0.298 kcal/mol [$=k_BT/2$ (T = 300 K)] and 46 points to the extent of 0.596 kcal/mol [$=k_BT$ (T = 300 K)] at each point on the IRC, i.e., 2236 points in total [22 × 46 × 2 + 22 (at each point on the IRC) + 190 (along the IRC)].[29]

For the interaction potential energy functions V_1^{int} and V_2^{int}, we have generated 1400 geometries by random deployment of positional and orientational coordinates of a water molecule within 7.5 Å of the center of mass of the ZW and NF, respectively.[8−10,23,35] Furthermore, we have obtained each 10 optimized geometries with respect to the relative distance and orientation between glycine (ZW or NF) and water. Namely, two sets of sample points for the ZW and NF consist of 1410 points, each.

TABLE 1: Optimized Parameters for the AMBER Potential Functions (Eq 2.7)[a]

ZW					NF				
	K_r	r_{eq}		K_ϕ		K_r	r_{eq}		K_ϕ
1-2[b]	0.388	1.762	1-2-34	0.104	1-2	0.524	1.460	1-2-3-4	0.034
1-6	0.370	0.985	1-2-3-5	0.163	1-7	0.664	0.997	1-2-3-5	−0.004
1-7	0.734	1.017	3-2-1-6	0.220	1-8	0.664	0.997	2-3-5-6	0.074
1-8	0.734	1.017	3-2-1-7	0.006	2-3	0.416	1.595	3-2-1-7	−0.007
2-3	0.293	1.854	3-2-1-8	0.005	2-9	0.631	1.094	3-2-1-8	−0.007
2-9	0.658	1.079	4-3-2-9	−0.019	2-10	0.631	1.094	4-3-5-6	0.046
2-10	0.658	1.079	4-3-2-10	−0.019	3-4	1.705	1.187	4-3-2-9	−0.019
3-4	1.402	1.256	5-3-2-9	−0.006	3-5	0.707	1.359	4-3-2-10	−0.019
3-5	0.817	1.247	5-3-2-10	−0.006	5-6	0.976	0.950	5-3-2-9	−0.014
	K_θ	θ_{eq}[d]	6-1-2-9	−0.038		K_θ	θ_{eq}	5-3-2-10	−0.014
1-2-3	0.399	2.277	6-1-2-10	−0.038	1-2-3	0.107	2.256	7-1-2-9	0.013
1-2-9	0.092	1.689	7-1-2-9	−0.007	1-2-9	0.069	2.009	7-1-2-10	0.013
1-2-10	0.092	1.689	7-1-2-10	0.011	1-2-10	0.069	2.009	8-1-2-9	0.013
2-1-6	0.085	2.831	8-1-2-9	0.011	2-1-7	0.090	1.944	8-1-2-10	0.013
2-1-7	0.096	1.934	8-1-2-10	−0.008	2-1-8	0.090	1.944		
2-1-8	0.096	1.934			2-3-4	0.137	2.551		
2-3-4	0.101	2.830			2-3-5	0.128	2.890		
2-3-5	0.096	3.499			3-2-9	0.096	1.935		
3-2-9	0.090	1.775			3-2- 10	0.096	1.935		
3-2-10	0.090	1.773			3-5-6	0.106	2.198		
4-3-5	0.167	2.791			4-3-5	0.122	2.625		
6-1-7	0.068	1.868			7-1-8	0.082	1.833		
6-1-8	0.068	1.869			9-2-10	0.064	1.830		
7-1-8	0.072	1.750				A	B	C	
9-2-10	0.067	1.583			1-6	2.67×10^{-9}	0.492	−0.272	
	A	B	C		4-7	2.00×10^{-3}	−54.701	0.227	
4-6	1.96×10^{-7}	16.628	−1.698		4-8	6.63×10^{-4}	−54.701	0.227	
4-7	2.82×10^{-2}	−29.389	0.071		5-7	6.94×10^{-5}	16.910	−0.243	
4-8	1.47×10^{-1}	−29.826	0.080		5-8	3.23×10^{-5}	16.910	−0.243	
5-6	1.55×10^{-14}	0.115	−0.253		6-7	5.64×10^{-6}	−1.013	0.077	
5-7	6.74×10^{-7}	17.864	−0.573		6-8	2.57×10^{-7}	−1.013	0.077	
5-6	1.34×10^{-6}	17.737	−0.568		6-9	1.17×10^{-6}	1 .733	−0.209	
					6-10	3.29×10^{-6}	1 .733	−0.209	

[a] K_r, r_{eq}, K_θ, θ_{eq}, K_ϕ, A, B, and C are given in units of hartree/Å^2, Å, hartree/rad^2, radian, hartree, hartree Å^{12}, hartree Å^6, and hartree Å, respectively. [b] The serial numbers 1, 2, 3, 4, and 5 correspond to a nitrogen, α-carbon, carbonyl carbon, carbonyl oxygen, and carbonyl oxygen atom accepting a transferring hydrogen atom, respectively. Further, 6, 7, and 8 denote hydrogen atoms connected with the nitrogen atom. 6 corresponds to the transferring hydrogen atom. 9 and 10 correspond to hydrogen atoms connected with the α-carbon atom.

Using the above conditions and the sample points, we have determined the disposable parameters by minimizing the sum of squares of the deviations Δ_{kk}^2, Δ_{12}^2, and Δ_k^{int2}:

$$\Delta_{kk}^2 = \Delta_{kk}^{E\,2} + \Delta_{kk}^{F\,2} = \frac{1}{N_k}\sum_i^{N_k}[V_{kk}(\mathbf{q}_i) - E_k(\mathbf{q}_i)]^2 + \frac{\Delta L^2}{N_k}\sum_{\partial V_{kk}}^{\partial \mathbf{q}}\left[-\frac{\partial V_{kk}}{\partial \mathbf{q}}(\mathbf{q}_i) - \mathbf{F}_k(\mathbf{q}_i)\right]^2 \quad (k = 1,2) \quad (2.12)$$

where $E_k(\mathbf{q}_i)$ is the total electronic energy at the ith sample geometry $\mathbf{q}_i$, N_k is the number of total sample points, ΔL is a weighting parameter for force, and $\mathbf{F}_k(\mathbf{q}_i)$ is the force vector at the ith sample geometry,

$$\Delta_{12}^2 = \frac{1}{N_{12}}\sum_i^{N_{12}}[V_{12}^2(\mathbf{q}_i) - (E(\mathbf{q}_i) - V_{11}(\mathbf{q}_i))\cdot(E(\mathbf{q}_i) - V_{22}(\mathbf{q}_i))]^2 \quad (2.13a)$$

$$\approx \frac{1}{N_{12}}\sum_i^{N_{12}}[(E(\mathbf{q}_i) - V_{11}(\mathbf{q}_i))\cdot(E(\mathbf{q}_i) - V_{22}(\mathbf{q}_i))]^2 \times [\ln V_{12}^2(\mathbf{q}_i) - \ln\{(E(\mathbf{q}_i) - V_{11}(\mathbf{q}_i))\cdot(E(\mathbf{q}_i) - V_{22}(\mathbf{q}_i))\}]^2 \quad (2.13b)$$

where $E(\mathbf{q}_i)$ is the total electronic energy at the ith sample geometry $\mathbf{q}_i$, N_{12} is the number of total sample points, and

$$\Delta_k^{int2} = \frac{1}{N_k^{int}}\sum_i^{N_k^{int}}[Vk^{int}(\mathbf{q}_i,\mathbf{R}_i) - E_k^{int}(\mathbf{q}_i,\mathbf{R}_i)]^2 \quad (2.14)$$

where $E_k^{int}(\mathbf{q}_i,\mathbf{R}_i)$ is the interaction energy at the ith sample geometry and N_k^{int} is the number of total sample points.

Finally, ΔL was determined to be 0.05 Å as Δ_{kk}^E is of the same order of Δ_{kk}^F. Further, in order to linearize the least-squares problem, we have used eq 2.13b. We have used a modified Levenberg−Marquardt method[43] in order to solve the nonlinear least squares minimization problems. The optimized parameters in these functions are available from the authors. In particular, the values of the parameters corresponding to eq 2.7 are shown in Table 1.

C. MD Simulation. Integration of the equation of motion was performed with the velocity Verlet method,[44] using the RATTLE algorithm[45] in order to constrain the internal coordinates for both water and glycine. The number of molecules in the simulation cube with one side length of 18.6 Å was 1 glycine and 213 water molecules. The mass density was set to be 0.997 g/cm^3, which corresponds to that of glycine−water solution (0.46 mol % = 1.9 wt %) at 300 K. We have calculated not only the solvent−solvent long-range Coulomb interaction but also the solute−solvent one using the Ewald sum technique[46] as follows

$$V^{C(1)}{}_{SS} = \frac{e^2}{8\pi\epsilon_0 L}\sum_{i\neq j}\frac{Z_i Z_j \cdot \mathrm{erfc}(\alpha_{SS} r_{ij}^*)}{r_{ij}^*} \quad (2.15)$$

$$V_{SS}^{C(2)} = \frac{e^2}{8\pi^2\epsilon_0 L}\sum_{h\neq 0}\frac{\exp(-\pi^2\mathbf{h}^2/\alpha_{SS}^2)}{\mathbf{h}^2}[\{\sum_i Z_i \cos(2\pi\mathbf{h}\cdot\mathbf{r}_i^*)\}^2 + \{\sum_i Z_i \sin(2\pi\mathbf{h}\cdot\mathbf{r}_i^*)\}^2] \quad (2.16)$$

$$V^{C(3)}{}_{SS} = -\frac{\alpha_{SS} e^2}{4\pi^{3/2}\epsilon_0 L}\sum_i Z_i^2 \quad (2.17)$$

for the solvent−solvent and

$$V_k^{intC(1)} = \frac{e^2}{4\pi\epsilon_0 L}\sum_i^R\sum_j^S \frac{Z_i^{(k)} Z_j \cdot \mathrm{erfc}(\alpha_{RS} r_{ij}^*)}{r_{ij}^*} \quad (2.18)$$

$$V_k^{intC(2)} = \frac{e^2}{4\pi^2\epsilon_0 L}\sum_{h\neq 0}\frac{\exp(-\pi^2\mathbf{h}^2/\alpha_{RS}^2)}{\mathbf{h}^2}\times [\sum_i^R Z_i^{(k)}\cos(2\pi\mathbf{h}\cdot\mathbf{r}_i^*)\sum_j^S Z_j\cos(2\pi\mathbf{h}\cdot\mathbf{r}_j^*) + \sum_i^R Z_i^{(k)}\sin(2\pi\mathbf{h}\cdot\mathbf{r}_i^*)\sum_j^S Z_j\sin(2\pi\mathbf{h}\cdot\mathbf{r}_j^*)] \quad (2.19)$$

for the ZW-solvent ($k = 1$) and NF-solvent ($k = 2$), respectively, where e, ϵ_0, Z_i, and Z_j are the elementary electric charge, the dielectric constant for vacuum, and the charges of the ith and jth atoms, respectively. $\mathbf{r}_i^*$ denotes such a scaled position as $\mathbf{r}_i/L$ where $\mathbf{r}_i$ and L are the position of the ith atom and the length of one side of the box, respectively. The reciprocal vector $\mathbf{h}$ is defined as (h_x, h_y, h_z), where h_x, h_y, and h_z are integers. The summations were truncated at $\mathbf{h}^2 = 17$, and then, we have chosen 2.5 and 4.0 for α_{SS} and α_{RS}, respectively. In order to make the force calculations manageable, we have employed the potential truncation technique[47] for the Lennard-Jones potential terms of both solvent−solvent and solute−solvent interaction energies, owing to the fast falling off of the corresponding forces. $L/2$ was chosen as the cutoff distance, because the forces for the Lennard-Jones potential terms were found to be almost zero at this distance. Equilibrium MD calculations of 10−20 ps were performed, after 15 ps cooling and equilibration runs with a time step of 0.5 fs. No temperature control algorithm was used to obtain the temperature range 302.4 ± 9.6 K.

D. Free Energy Perturbation Theory. MD calculations were performed to obtain the free energy surface on which the intramolecular proton transfer reaction of glycine proceeds. The free energy perturbation theory[33−36] provided the free energy change as the IRC, s, was varied in increments, Δs_i ($i = 1, ..., 27$) from $s = -0.388$ to $s = 1.50$ amu$^{1/2}$ a_0. Specifically, the free energy change for moving s_i to $s_{i+1} = s_i + \Delta s_i$ is given by eq 2.20 as follows

$$G_{i+1} - G_i = -k_B T \ln\langle\exp[-\beta\{V_{RS}(s_{i+1}) - V_{RS}(s_i)\}]\rangle_i \quad (2.20)$$

where $\beta = 1/k_B T$, $V_{RS}(s_{i+1}) - V_{RS}(s_i)$ is the energy difference between the systems with s_{i+1} and s_i, and the average is based on sampling for s_i. Naturally, if the reference, s_i, and perturbed, s_{i+1}, systems are too disparate, convergence of the average in eq 2.20 will be slow. As shown below, choosing Δs_i larger than 0.01 amu$^{1/2}$ a_0 and less than 0.10 amu$^{1/2}$ a_0 was not problematic in the present calculations.

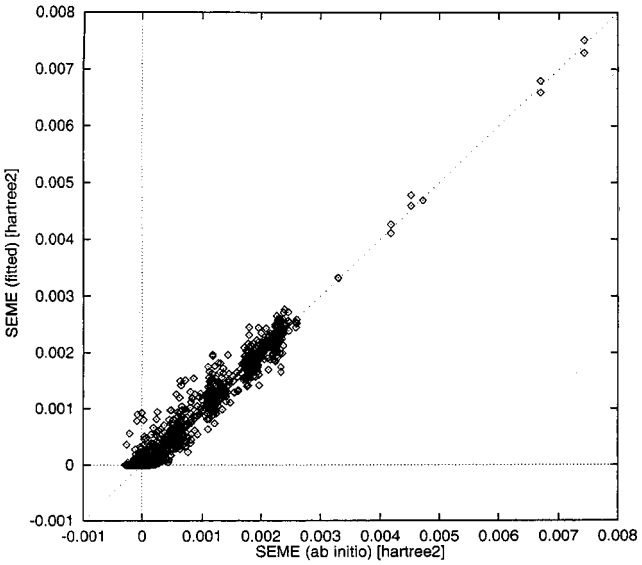

Figure 2. SEME calculated by the optimized parameters and its corresponding quantum mechanically calculated values at all sample points.

III. Results and Discussion

A. The Potential Function Fitting. According to the procedures shown in section II, we have determined the disposable parameters. In Figure 1, the fitted SEMEs by the CM's and our procedures are shown with its quantum mechanically calculated values along the IRC. The abscissa indicates the IRC: the origin corresponds to the TS in the gas phase, the negative side corresponds to the ZW, and the positive side to the NF. Around the TS, the CM's SEME reproduces the quantum mechanical values very well, while there are small differences between theirs and ours. However, in the course of the reaction, the CM's SEME deviates from the *ab initio* data very largely, and it is found that our procedure has improved quite well the values of the SEME. Figure 2 shows the correlation between the fitted SEME and its *ab initio* values with respect to all sample points. It is found that the fitted SEME reproduces the *ab initio* values not only along the IRC but also at all sample points. The standard deviations Δ_{11}^E, Δ_{11}^F, Δ_{22}^E, Δ_{22}^F, Δ_1^{int}, and Δ_2^{int} are 1.14×10^{-4}, 6.99×10^{-4}, 1.07×10^{-4}, 6.09×10^{-4}, 4.77×10^{-4}, and 4.48×10^{-4} hartree, respectively. For the standard deviation of the SEME Δ_{12}, we have obtained the value of 1.30×10^{-4} hartree^2.

For investigation of the quality of the fitted potential function, we have plotted the values of V_R in eq 2.3 vs those by the *ab initio* method along the IRC in Figure 3 and found that the fitted potential function reproduces the potential energy profile along the IRC. In particular, although the barrier height of the reaction in the gas phase due to the *ab initio* method is extremely small (8.97×10^{-4} hartree = 0.563kcal/mol), the fitted function reproduces satisfactorily the barrier height. In Figure 4, the correlation between the values of the fitted potential function and the corresponding *ab initio* values with respect to all sample points is shown. It is found that the values of the fitted function are in good agreement with *ab initio* values not only along the IRC but also in the vicinity of the IRC; i.e., the standard deviation is 7.40×10^{-4} hartree (0.464 kcal/mol).

B. Interaction Energy between Glycine and Water Molecules. We have shown how well the potential functions,

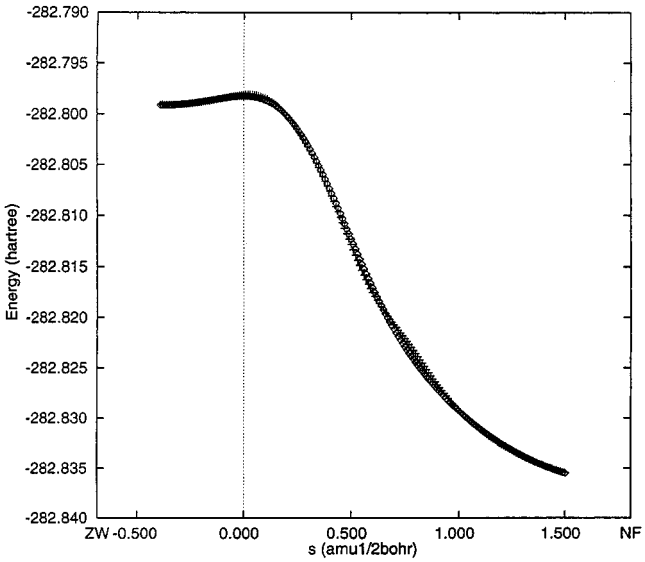

Figure 3. Potential energies calculated by the optimized potential function V_R (plus) and their corresponding quantum mechanically calculated values (open diamond). The abscissa is the IRC.

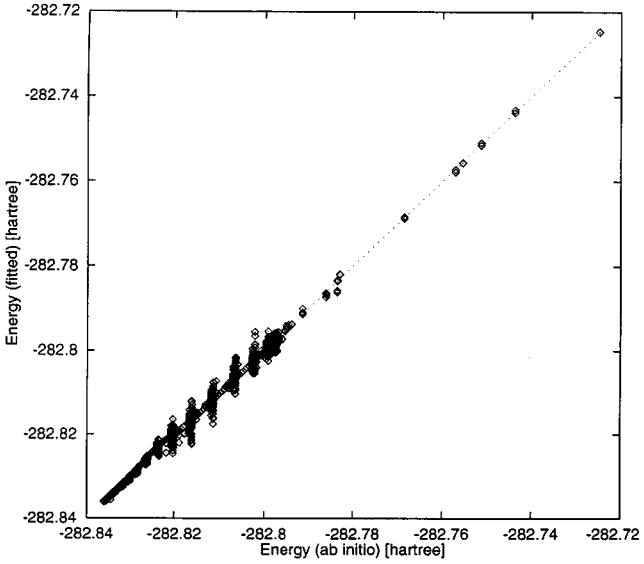

Figure 4. Energy correlation between the optimized potential function V_R and its corresponding *ab initio* calculation.

especially, the SEME and V_R, are fitted to the *ab initio* data. However, to what extent the interaction potential functions reproduce the *ab initio* data has not been shown, except for the standard deviations, i.e., Δ_1^{int} and Δ_2^{int}. For an examination of the quality of the fitted interaction potential functions, let us estimate the average of the interaction energy along the IRC by carrying out MD simulations. In Figure 5, $\langle V_R - V_{RS}\rangle$, $\langle V_R\rangle$, and $\langle V_{RS}\rangle$, which denote the averages of $V_R - V_{RS}$, V_R, and V_{RS}, respectively, are shown along the IRC. $\langle V_R - V_{RS}\rangle$ at the ZW and NF are 66.83 ± 13.28 and 23.11 ± 9.32 kcal/mol, respectively. This means that the ZW is much more stable than the NF in aqueous solution. Furthermore, there seems a mound in the energy profile of $\langle V_{RS}\rangle$ with a barrier height of ~30 kcal/mol at $s \approx 0.6$ amu$^{1/2}$ a_0. The monotonous decrease of $\langle V_R - V_{RS}\rangle$ and the stability increase of the solute in the course of the reaction are compensated by each other, and the offset results in the barrier around the point. It may also suggest that the TS on the free energy surface is located around the point, if the entropy contribution to the free energy of activation is small. To determine the location of the TS on the free energy surface

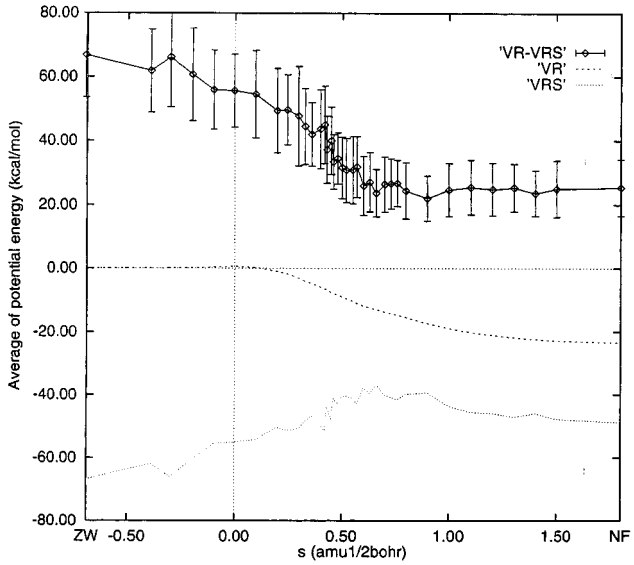

Figure 5. Averages of the interaction energies along the IRC: $\langle V_R - V_{RS}\rangle$ (solid curve with error bars), $\langle V_R\rangle$ (dashed curve), and $\langle V_{RS}\rangle$ (dotted curve).

exactly, we should calculate the free energy surface by the free energy perturbation theory, as shown later.

Clementi *et al.*[8−10] obtained the corresponding interaction energies of 99.14 ± 1.19 and 12.78 ± 0.19 kcal/mol by MC simulations using different glycine−water interaction potentials and water−water potential functions. Both theirs and the present result predict the ZW to be much more stable than NF. However, there are appreciable quantitative differences. They may be attributed to (1) the difference of the glycine−water interaction potential functions, (2) the water−water interaction potential functions, or (3) the averaging methods. With respect to the analytical form of the glycine−water interaction potential function, both are the same. However, the basis set[8−10] used to calculate the interaction energies is different from ours (6-31+G*), and the standard deviation of the interaction energies is 0.60 kcal/mol in comparison to 0.30 kcal/mol for ours. Therefore, our function should be in better agreement with the *ab initio* data than theirs. However, it does not necessarily mean that our function reproduces the average of the interaction energy better than theirs.

With respect to the water−water potential, they used the Matsuoka−Clementi−Yoshimine (MCY) potential function.[48] According to Neumann,[40] the static dielectric constant of the TIP4P−water is $\epsilon_0 = 53$ at 293 K, while that of the MCY model is $\epsilon_0 = 34$ at 292 K. Owing to it, we can apparently guess that the TIP4P−water should interact with the ZW stronger than the MCY−water. However, this conflicts with both our result and theirs. If the guess is true, we should consider that the difference in those water−water potential functions has little effect on the averages of the interaction energy, but that in the glycine−water interaction potentials mainly contributes to them.

With respect to the averaging methods, in order to calculate the average of the interaction energy, we have employed the MD method with 4×10^4 time steps, while they have used the MC method with 10^6 MC steps.[8−10] Our standard deviation of the interaction energy is larger than theirs due to the difference in the numbers of MD and MC steps. Taking this into account, it seems that there are still appreciable discrepancies.

According to the above discussion, the differences of the water−water interaction potential functions and the averaging methods do not influence the averages of the interaction energy

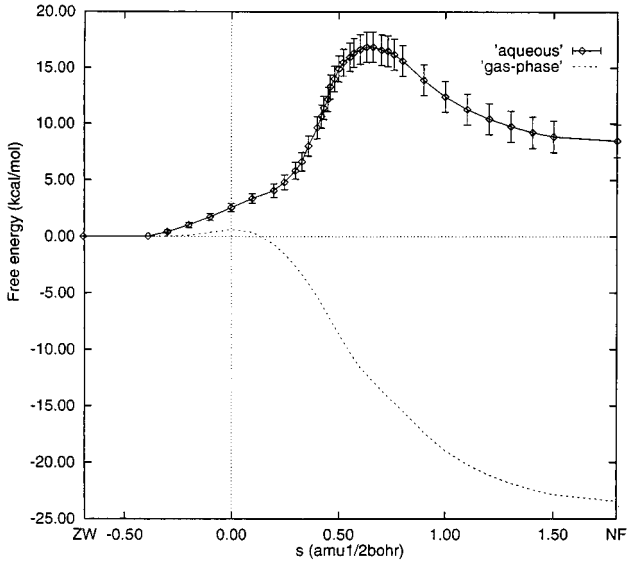

Figure 6. Free energy difference in aqueous solution (solid curve with error bars) and the potential energy in the gas phase V_R (dashed curve). The abscissa is the IRC.

very much, but that of the glycine−water interaction potentials does. Since our interaction potentials at the ZW and NF have the same forms as those which Clementi *et al.* have developed (V_{12}^2 is approximately equal to zero at the ZW and NF), it can be concluded that the inconsistency are due to difference between their and our basis sets.

C. Free Energy Change. In order to confirm whether our function could describe statistical and thermodynamic quantities well or not, a comparison should be made between calculated and experimental values. However, experimental values corresponding to the interaction energy do not exist. Therefore, on the assumption of equilibrium solvation, we have compared both the free energy change of the reaction and the free energy of activation with the experimental values. In Figure 6, free energy changes along the IRC are shown. It is found that the TS on the free energy curve approximately corresponds to the geometry at $s \approx 0.66$ amu$^{1/2}$ a_0 in the IRC of the gas phase, which is clearly consistent with the location of the mound in $\langle V_{RS} \rangle$. The free energy difference between the ZW and NF is 8.46 ± 1.45 kcal/mol and the free energy of activation is 16.85 ± 1.36 kcal/mol from the ZW side. Because the corresponding experimental values are 7.27 and 14.36 kcal/mol, respectively,[7,16] the present results are found to be in good agreement with them. It means that our fitted potential function can describe very well not only the internal energy of glycine but also the interaction with water, the free energy difference of the reaction, and then the free energy of activation. If the equilibrium solvation is not realized, our results cannot be directly compared with the experimental ones. However, the agreement with them should support positively the assumption of equilibrium solvation in the glycine−water reaction system.

IV. Summary

In this paper, by using the EVB method with the exchange matrix element improved by Chang and Miller to reproduce an *ab initio* surface with high accuracy, an analytical potential function of the glycine−water system has been presented. The analytical potential function can describe not only its reactive potential energy surface but also the interaction energy with water. Fitting the present potential function to the *ab initio* data sampled at various points in the neighborhood along the IRC, it was shown that the function can reproduce satisfactorily the Born−Oppenheimer adiabatic surface.

For an examination of the quality of the fitted interaction potential function, we calculated along the IRC the average of the glycine−water interaction energy in the intramolecular proton transfer reaction and obtained 66.83 and 23.11 kcal/mol for the interaction energies at the ZW and NF, respectively. Our result predicts the ZW to be much more stable than the NF, which is consistent with that of Clementi *et al.*

For the purpose to confirm that our potential function can reproduce the thermodynamic quantities, we presented the free energy change along the IRC, by using the free energy perturbation theory. It was found that the TS on the free energy surface corresponds clearly to the geometry at $s \approx 0.66$ amu$^{1/2}$ a_0 on the IRC of the gas phase. The free energy difference between ZW and NF is 8.46 ± 1.45 kcal/mol and the free energy of activation is 16.85 ± 1.36 kcal/mol, which are both in good agreement with the experimental values, respectively. We conclude that our fitted potential function can reproduce not only the internal energy of glycine but also the interaction with water, the free energy difference of the reaction, and then the free energy of activation.

By utilizing the present potential function, we can first understand the origin of the barrier in aqueous solution by estimating the temperature dependence of the free energy of activation and the solvation structure difference of glycine at the TS and the minima (ZW and NF). Second, carrying out MD simulations including the internal degrees of freedom of glycine, we can estimate how far from equilibrium the non-equilibrium distribution of the solvents is and to what extent the distribution influences the rate constant. These studies will be carried out in the near future.[49]

Acknowledgment. The authors thank Professor Kenichi Fukui for his helpful advice and discussion. They also thank Dr. Y. Okuno for stimulating and fruitful discussion. The numerical calculations were carried out by using the NEC SX-4 at the Institute for Fundamental Chemistry and computers at the Institute for Molecular Science. This work was supported by a Grant-in-Aid for Science Research from the Ministry of Education, Science, and Culture in Japan, and financially by the Research for the Future Program of the Japan Society for the Promotion of Science (Project No. JSPS-RFTF96P00206).

References and Notes

(1) Schuster, P.; Wolschann, P.; Tortschanoff, K. Dynamics of proton transfer in solution. In *Chemical relaxation in molecular biology*; Pecht, I., Rigler, R., Eds.; Springer−Verlag: Berlin, Heidelberg, 1976.

(2) Morrison, R. T.; Boyd, R N. *Organic Chemistry,* 4th ed.; Allyn and Bacon, Inc.: Boston, MA, 1983.

(3) Tse, Y.-C.; Newton, M. D.; Vishveshwara, S.; Pople, J. A. *J. Am. Chem. Soc.* **1978**, *100*, 4329.

(4) Ding, Y.; Krogh-Jespersen, K. *Chem. Phys. Lett*. **1992**, *199*, 261; *J. Comput. Chem.* **1996,** *17*, 338.

(5) Yu, D.; Armstrong, D. A.; Rauk, A. *Can. J. Chem.* **1992,** *70*, 1762.

(6) Jensen, J. H.; Gordon, M. S. *J. Am. Chem. Soc*. **1995,** *117*, 8159.

(7) Wada, G.; Tamura, E.; Okina, M.; Nakamura, M. *Bull. Chem. Soc. Jpn.* **1982**, *55*, 3064.

(8) Romano, S.; Clementi, E. *Int. J. Quantum Chem.* **1978,** *14*, 839.

(9) Clementi, E.; Cavallone, F.; Scordamaglia, R. *J. Am. Chem. Soc.* **1977,** *99*, 5531.

(10) Carozzo, L.; Corongiu, G.; Petrongolo, C.; Clementi, E. *J. Chem. Phys.* **1978**, *68*, 787.

(11) Sheinblatt, M.; Gutowsky, H. S. *J. Am. Chem. Soc.* **1964,** *86*, 4814.

(12) Chang, K. C.; Grunwald, E. *J. Phys. Chem.* **1976,** *80*, 1422.

(13) Slifkin, M. A.; Ali, S. M. *J. Mol. Liq.* **1984**, *28*, 215.

(14) Inoue, H. *J. Sci. Hiroshima Univ. Ser. A-II* **1970**, *34*, (1), 17.

(15) Applegate, K.; Slutsky, L. J.; Parker, R. C. *J. Am. Chem. Soc.* **1968**, *90*, 6909.

(16) Hussey, M.; Edmonds, P. D. *J. Acoust. Soc. Am.* **1971**, *49*, 1309.
(17) (a) Eyring, H. *J. Chem. Phys.* **1934**, *3*, 107. (b) Wigner, E. *J. Chem. Phys.* **1937**, *5*, 720.
(18) Truhlar, D. G.; Hase,W. L.; Hynes, J. T. *J. Phys. Chem.* **1983**, *87*, 2664.
(19) Glasstone, S.; Laidler, K. J.; Eyring, H. *The Theory of Rate Processes*; McGraw-Hill: New York, 1941.
(20) Hänggi, P.; Talkner, P.; Borkovec, M. *Rev. Mod. Phys.* **1990**, *62*, 251 and references therein.
(21) Hynes, J. T. In *Theory of Chemical Reaction Dynamics*; Baer, M., Ed.; CRC Press: Boca Raton, FL, 1985; Vol. IV and references therein.
(22) (a) Nagaoka, M.; Yoshida, N.; Yamabe, T. *J. Mol. Liq.* **1995**, *65/66*, 289. (b) Nagaoka, M.; Yoshida, N.; Yamabe, T. *J. Chem. Phys.* **1996**, *105*, 5431. (c) Nagaoka, M.; Okuno, Y.; Yamabe, T. *J. Chem. Phys.* **1992**, *97*, 8143. (d) Nagaoka, M.; Okuno, Y.; Yamabe, T. To be submitted. (e) Nagaoka, M.; Okuno, Y.; Yoshida, N.; Yamabe, T. *Int. J. Quantum Chem.* **1994**, *51*, 519. (f) Nagaoka, M.; Yoshida, N.; Yamabe, T. *Int. J. Quantum Chem.* **1996**, *60*, 287. (g) Okuno, Y. Dissertation; Kyoto University, 1992.
(23) Nagaoka, M.; Okuno, Y.; Yamabe, T. *J. Phys. Chem.* **1994**, *98*, 12506.
(24) (a) Sumi, H. *J. Phys. Chem.* **1991**, *95*, 3334. (b) Sumi, H.; Marcus, R. A. *J. Chem. Phys.* **1986**, *84*, 4894. (c) Sumi, H.; Asano, T. *J. Chem. Phys.* **1995**, *102*, 9565.
(25) Hayashi, S.; Ando, K.; Kato, S. *J. Phys. Chem.* **1995**, *99*, 955.
(26) (a) Vishveshwara, S.; Pople, J. A. *J. Am. Chem. Soc.* **1977**, *99*, 2422. (b) Jensen, J. H.; Gordon, M. S. *J. Am. Chem. Soc.* **1991**, *113*, 7917. (c) Császár, A. G. *J. Am. Chem. Soc.* **1992**, *114*, 9568. (d) Hu, C.-H.; Shen, M.; Schaefer, H. F. III. *J. Am. Chem. Soc.* **1993**, *115*, 2923. (e) Frey, R. F.; Coffin, J.; Newton, S. Q.; Ramek, M.; Cheng, V. K. W.; Momany, F. A.; Schäfer, L. *J. Am. Chem. Soc.* **1992**, *114*, 5369. (f) Godfrey, P. D.; Brown, R. D. *J. Am. Chem. Soc.* **1995**, *117*, 2019. (g) Barone, V.; Adamo, C.; Lelj, F. *J. Chem. Phys.* **1995**, *102*, 364.
(27) (a) Bonaccorsi, R., Palla, P.; Tomasi, J. *J. Am. Chem. Soc.* **1984**, *106*, 1945. (b) Kikuchi, O.; Natsui, T.; Kozaki, T. *J. Mol. Struct.* THEOCHEM **1990**, *207*, 103. (c) Iglesias, E.; Sordo, T. L.; Sordo, J. A. *J. Mol. Struct.* THEOCHEM **1994**, *309*, 81. (d) Imamura, A.; Fujita, K.; Nagata, C. *Bull. Chem. Soc. Jpn.* **1969**, *42*, 3118.
(28) (a) Murrell, J. N.; Carter, S.; Farantos, S. C.; Huxley, P.; Varandas, A. J. C. *Molecular Potential Energy Functions*; Wiley: New York, 1984 (b) Bergsma, J. P.; Gertner, B. J.; Wilson, K. R.; Hynes, J. T. *J. Chem. Phys.* **1987**, *86*, 1356.
(29) Nagaoka, M.; Okuno, Y.; Yamabe, T.; Fukui, K. *Int. J. Quantum Chem.* **1992**, *42*, 889.
(30) (a) Warshel, A.; Weiss, R. M. *J. Am. Chem. Soc.* **1980**, *102*, 6218. (b) Åqvist, J.; Warshel, A. *Chem. Rev.* **1993**, *93*, 2523. (c) Warshel, A. *Computer Modeling of Chemical Reactions in Enzymes and Solutions*; John Wiley and Sons, Inc.: New York, 1991. (d) Warshel, A.; Russell, S. J. *Am. Chem. Soc.* **1986**, *108*, 6569. (e) Hwang, J.-K.; King, G.; Creighton, S.; Warshel, A. *J. Am. Chem. Soc.* **1988**, *110*, 5297.
(31) (a) Chang, Y.-T.; Miller, W. H. *J. Phys. Chem.* **1990**, *94*, 5884. (b) Miller, W. H.; Chang, Y.-T.; Makri, N. *Molecular Structure and Reactivity* in *Computational Advances in Organic Chemistry*; Ögretir, C., Csizmadia, I. G., Eds.; Kluwer Academic Publishers: Netherlands, 1991.
(32) Pauling, L. *The Nature of the Chemical Bond*; Cornell University Press: Ithaca, NY, 1960. Coulson, C. A.; Danielsson, U. *Ark. Fys.* **1954**, *8*, 239.
(33) Zwanzig, R. W. *J. Chem. Phys*. **1954**, *22*, 1420.
(34) Torrie, G. M.; Valleau, J. P. *Chem. Phys. Lett.* **1974**, *28*, 578.
(35) (a) Jorgensen, W. L.; Ravimohan, C. *J. Chem. Phys.* **1985**, *83*, 3050. (b) Jorgensen, W. L.; Buckner, J. K. *J. Phys Chem.* **1987**, *91*, 6083. (c) Jorgensen, W. L.; Gao, J. *J. Am. Chem. Soc.* **1988**, *110*, 4212. (d) Jorgensen, W. L. *Adv. Chem. Phys.* **1988**, *70*, 469. (e) Jorgensen, W. L. *Acc. Chem. Res.* **1989**, *22*, 184. (f) Duffy, E. M.; Severance, D. L.; Jorgensen, W. L. *J. Am. Chem. Soc.* **1992,** *114***,** 7535.
(36) (a) Singh, U. C.; Brown, F. K.; Bash, P. A.; Kollman, P. A. *J. Am. Chem. Soc.* **1987**, *109*, 1607. (b) Kollman, P. *Chem. Rev.* **1993**, *93*, 2395. (c) Kollman, P. A.; Merz, JR. K. M. *Acc. Chem. Res.* **1990**, *23*, 246.
(37) (a) Fukui, K. *J. Phys. Chem.* **1970**, *74*, 461; (b) *Acc. Chem. Res.* **1981**, *14*, 363; (c) In *The World of Quantum Chemistry*; Daudel, R., Pullman, B., Eds.; Reidel: Dordrecht, 1974.
(38) (a) Swaminathan, S.; Whitehead, R. J.; Guth, E.; Beveridge, D. L. *J. Am. Chem. Soc.* **1977**, *99*, 7817. (b) Jorgensen, W. L.; Cournoyer, M. E. *J. Am. Chem. Soc.* **1978**, *100*, 4942. (c) Alper, J. S.; Dothe, K.; Coker, D. F. *Chem. Phys.* **1991**, *153*, 51. (d) Ando, K.; Kato, S. *J. Chem. Phys.* **1991**, *95*, 5966.
(39) (a) Jorgensen, W. L.; Chandrasekher, J.; Madura, J. D.; Impey, R. W.; Klein, M. L. *J. Chem. Phys.* **1983**, *79*, 926. (b) Jorgensen, W. L.; Madura, J. D. *Mol. Phys.* **1985**, *56*, 1381.
(40) Neumann, M. *J. Chem. Phys.* **1986**, *85*, 1567.
(41) Frisch, M. J.; Trucks, G. W.; Head-Gordon, M.; Gill, P. M. W.; Wong, M. W.; Foresman, J. B.; Johnson, B. G.; Schlegel, H. B.; Robb, M. A.; Replogle, E. S.; Gomperts, R.; Andres, J. L.; Raghavachari, K.; Binkley, J. S.; Gonzalez, C.; Martin, R. L.; Fox, D. J.; Defrees, D. J.; Baker, J.; Stewart, J. J. P.; Pople, J. A. *Gaussian92, Revision C.4*; Gaussian Inc.: Pittsburgh, PA, 1992.
(42) Miller, W. H.; Handy, N. C.; Adams, J. E. *J. Chem. Phys.* **1980**, *72*, 99.
(43) (a) Levenberg, K. *Q. Appl. Math.* **1994**, *2*, 164. (b) Marquardt, D. *J. Soc. Ind. Appl. Math.* **1963**, *11*, 431.
(44) (a) Verlet, L. *Phys. Rev.* **1967**, *159*, 98. (b) Swope, W. C.; Andersen, H. C.; Berens, P. H.; Wilson, K. R. *J. Chem. Phys.* **1982**, *76*, 637. (c) Humphreys, D. D.; Friesner, R. A.; Berne, B. J. *J. Phys. Chem.* **1994**, *98*, 6885.
(45) Andersen, H. C. *J. Comput. Phys.* **1983**, *52*, 24.
(46) Ewald, P. *Ann. Phys.* **1921,** *64*, 253.
(47) Allen, M. P.; Tildesley, D. J. *Computer Simulation of Liquids*; Oxford University Press: Oxford, 1987.
(48) Matsuoka, O.; Clementi, E.; Yoshimine, M. *J. Chem. Phys.* **1976,** *64*, 1351.
(49) Nagaoka, M.; Okuyama-Yoshida, N.; Yamabe, T. To be submitted.